ELSEVIER

Journal of Alloys and Compounds 356–357 (2003) 664–668

Journal of ALLOYS AND COMPOUNDS

www.elsevier.com/locate/jallcom

Hydrogen-induced transformations in C15 Laves phases $CeFe_2$ and $TbFe_2$ studied by pressure calorimetry up to 5 MPa

K. Aoki*, M. Dilixiati[1], K. Ishikawa

Department of Materials Science, Faculty of Engineering, Kitami Institute of Technology, 165 Koen-cho, Kitami, 090-8507 Hokkaido, Japan

Received 1 September 2002; accepted 30 December 2002

Abstract

Structural changes in C15 Laves phases $CeFe_2$ and $TbFe_2$ during thermal analysis in a hydrogen atmosphere (0.1~5.0 MPa) were examined using pressure differential scanning calorimetry (PDSC) in order to compare conditions of hydrogen-induced amorphization (HIA). In the pressure range investigated hydrogen absorption in $CeFe_2$ always gives rise to HIA and no crystalline (*c*-) $CeFe_2H_x$ hydride is formed. As the temperature increases, CeH_2 precipitates in amorphous (*a*-) $CeFe_2H_x$ and the remaining amorphous phase decomposes into CeH_2 and α-Fe. On the contrary, hydrogen absorption in $TbFe_2$ always leads to formation of *c*-$TbFe_2H_x$ hydride at near the room temperature. As the temperature increases, *c*-$TbFe_2H_x$ transforms to *a*-$TbFe_2H_x$ hydride, becomes *a*-$Tb_{1-y}Fe_2H_x+Tb_yH_2$ or decomposes directly into $TbH_2+\alpha$-Fe depending on the hydrogen pressure. As the temperature increases, TbH_2 precipitate in *a*-$TbFe_2H_x$ hydride and the remaining amorphous phases decompose into $TbH_2+\alpha$-Fe. The difference in the formation process of hydrogen-induced amorphous alloys between these compounds is discussed.

Keywords: Amorphous; Hydrogen; C15 Laves phase; Transformation; Crystallization; X-Ray diffraction

1. Introduction

Hydrogen-induced amorphization (HIA), i.e. the formation of amorphous phases by hydrogen absorption, is known to occur in intermetallic compounds with the C15, $L1_2$, $D0_{19}$, C23 and $B8_2$ structures containing a metal with high affinity to hydrogen [1–6]. Recently, the present authors have found out that structural changes in C15 Laves phases RFe_2 in 1.0 MPa H_2 depend on a kind of R [7,8]. That is, hydrogen absorption in a crystalline state, HIA, precipitation of RH_2 in an amorphous phase and decomposition of the remaining amorphous phase into RH_2 and α-Fe occur exothermally with increasing temperature in RFe_2 (R=Y, Sm, Gd, Tb, Dy and Ho). On the contrary, hydrogen absorption and HIA occur simultaneously in $CeFe_2$, while HIA and precipitation of ErH_2 do simultaneously in $ErFe_2$. Then, single-phase crystalline (*c*-) $CeFe_2H_x$ hydride and single-phase amorphous (*a*-) $ErFe_2H_x$ hydride are not formed in 1.0 MPa H_2. More recently, the present authors have reported that HIA depend strongly on the hydrogen pressure [9]. That is, HIA and precipitation of ErH_2 occurs separately above 2.0 MPa H_2, but *c*-$ErFe_2H_x$ hydride decomposes directly into $ErH_2+\alpha$-Fe at low hydrogen pressure. However, it is still unclear whether hydrogen absorption and HIA occurs separately in $CeFe_2$. In the present work, pressure dependence of structural changes in C15 Laves phases $CeFe_2$ and $TbFe_2$ during thermal analysis in a hydrogen atmosphere between 0.1 and 5.0 MPa is investigated in order to elucidate conditions of HIA and its mechanism.

2. Experimental

C15 Laves phases $CeFe_2$ and $TbFe_2$ were prepared by arc melting of high-purity metals (99.9% Fe, Ce and Tb) in a purified argon atmosphere. These alloy ingots were homogenized at 973 K for 1 week in an evacuated quartz tube. The ingot was pulverized (under 100 mesh) using a hand mill in acetone for preventing ignition and oxidation. Thermal analysis of these alloy powders (under 100 mesh) was carried out using pressure differential scanning calorimetry (PDSC) at heating rates of 0.17 and 0.33 K/s in a hydrogen (99.99999%) atmosphere of 0.1–5.0 MPa.

*Corresponding author.
E-mail address: aokiky@mail.kitami-it.ac.jp (K. Aoki).
[1]Graduate student, Kitami Institute of Technology.

0925-8388/03/$ – see front matter
doi:10.1016/S0925-8388(03)00148-8

The powder sample was evacuated at the room temperature and then hydrogen gas was introduced, that is, no activation treatment was done before thermal analysis. The origin of each thermal peak was determined by heating the samples to respective stages in PDSC followed by rapid cooling, and by subjecting them to powder X-ray diffraction (XRD), conventional DSC (Ar-DSC) in a flowing argon (99.999%) atmosphere and the hydrogen analysis. The hydrogen analysis was performed by the thermal conductivity method.

3. Results

Fig. 1 shows PDSC curves of $CeFe_2$ heated at hydrogen pressures of 1.0, 0.2 and 0.1 MPa at rates of 0.17 and 0.33 K/s and the change in the hydrogen content (H/M). Two or three exothermic peaks are seen in these PDSC curves. In this figure, arrows indicate the temperatures at which the heating was stopped and samples were rapidly cooled to identify the structural changes.

Figs. 2 and 3 show XRD patterns and Ar-DSC curves of $CeFe_2$, respectively, heated to the distinct stages in 0.2 MPa H_2 at a rate of 0.17 K/s. The hydrogen content of the sample heated to above the first exothermic peak (to 473 K) is 1.24 (H/M). The XRD pattern of this sample shows a broad peak, but does not show any Bragg peaks. Furthermore, the Ar-DSC curve of this sample shows two exothermic peaks of crystallization around 580 and 660 K. Consequently, we can see that hydrogen absorption gives rise to HIA in $CeFe_2$ at the first exothermic peak in Fig. 1. In the XRD pattern of the sample heated to 633 K, new

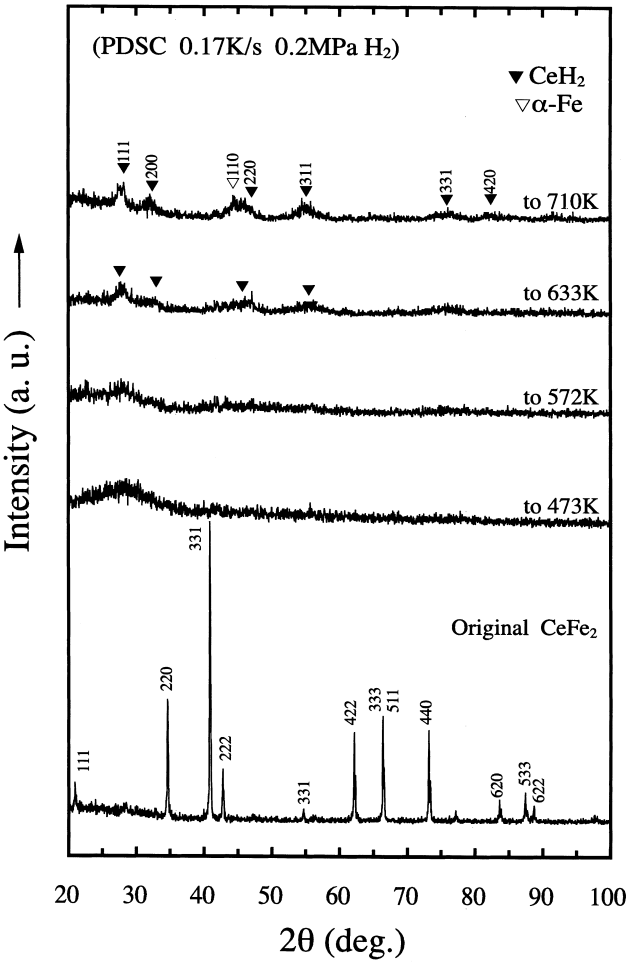

Fig. 2. XRD patterns of $CeFe_2$ after heating to respective stages of PDSC at a rate of 0.17 K/s and H_2 pressure of 0.2 MPa.

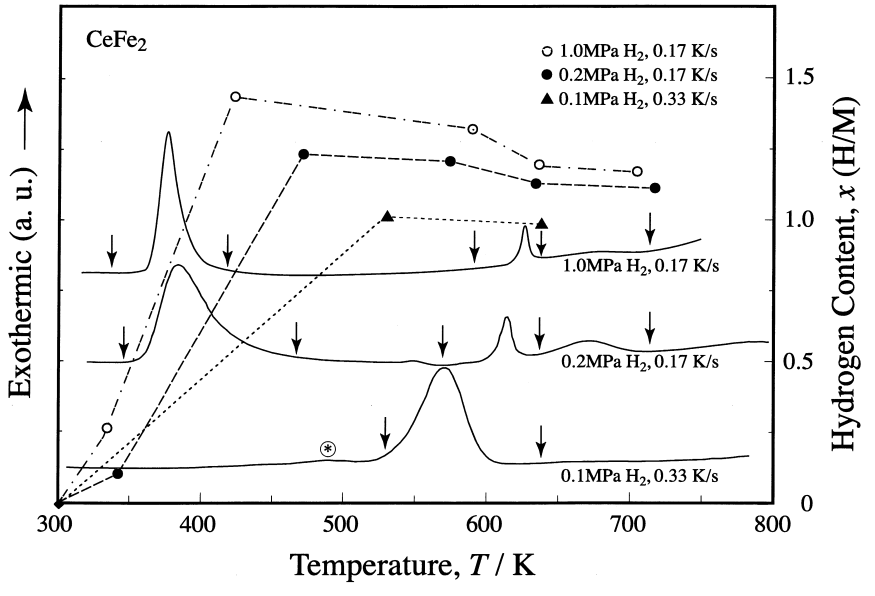

Fig. 1. PDSC curves of $CeFe_2$ heated at hydrogen pressures of 1.0, 0.2 and 0.1 MPa H_2 at rates of 0.17 and 0.33 K/s and the change in the hydrogen content (H/M).

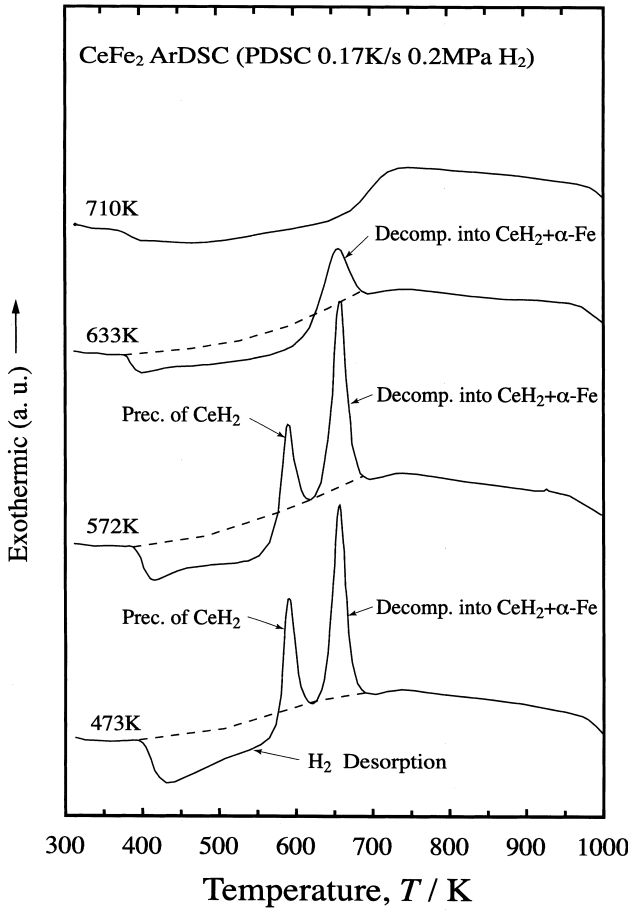

Fig. 3. Ar-DSC curves of $CeFe_2$ after heating to distinct stages of PDSC at a rate of 0.17 K/s and H_2 pressure of 0.2 MPa.

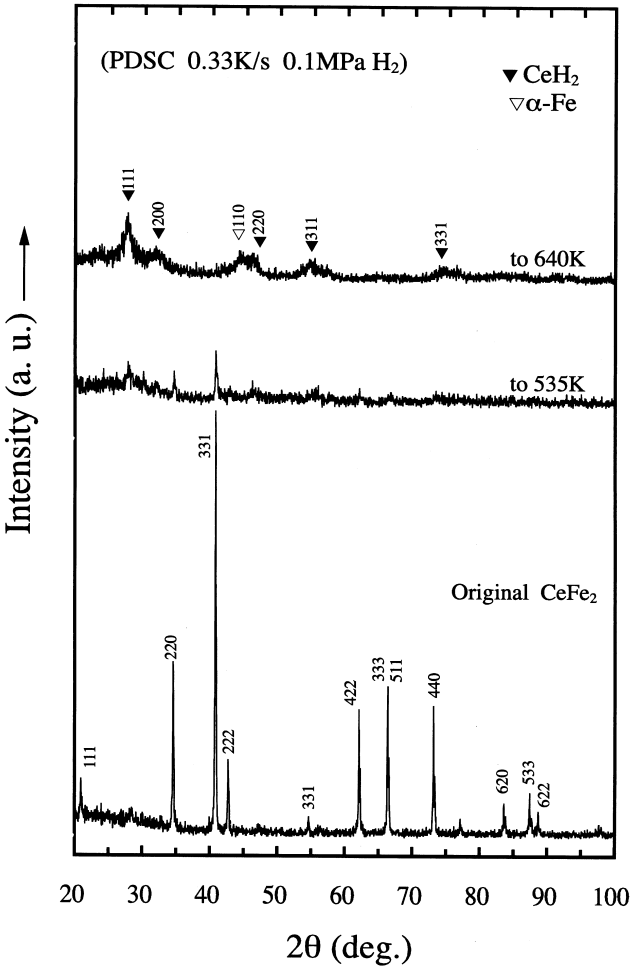

Fig. 4. XRD patterns of $CeFe_2$ heated at a rate of 0.17 K/s and at 0.2 MPa H_2.

broad Bragg peaks of CeH_2 appear overlapped with the broad peak. The Ar-DSC curve of this sample shows one exothermic peak of crystallization. Consequently, the second exothermic peak in PDSC is due to precipitation of CeH_2 in the amorphous phase. The XRD pattern of the sample heated to 710 K is indexed on the basis of CeH_2 and α-Fe and its Ar-DSC curve does not show any exothermic peak of crystallization. These observations indicate that the third exothermic peak in PDSC is due to decomposition of the remaining amorphous phase into CeH_2+α-Fe.

Fig. 4 shows XRD patterns of $CeFe_2$ heated to the distinct stages of PDSC in 0.1 MPa H_2 at a rate of 0.33 K/s. The XRD pattern of the sample heated to above very weak exothermic peak (to 535 K) shows small Bragg peaks of $CeFe_2$ overlapped with the broad peak. In addition, the Ar-DSC curve of this sample shows two exothermic peak of crystallization (not shown). The hydrogen content of this sample is 1.0 (H/M). Consequently, the weak first exothermic peak at around 480 K in PDSC is due to hydrogen absorption forming an amorphous phase. Since the Bragg peaks do not shift to the lower angle side as shown in Fig. 4, no *c*-$CeFe_2H_x$ hydride is formed in $CeFe_2$. The XRD pattern of the sample heated to 640 K in PDSC is indexed on the basis of CeH_2 and α-Fe. Consequently, the second prominent exothermic peak in PDSC is due to decomposition of *a*-$Ce_{1-y}Fe_2H_x$ into CeH_2+α-Fe. No *c*-$CeFe_2H_x$ hydride is detected under the present experimental conditions.

On the contrary, hydrogen absorption in $TbFe_2$ always leads to formation of *c*-$TbFe_2H_x$ hydride near room temperature [10]. On heating, *c*-$TbFe_2H_x$ transforms to *a*-$TbFe_2H_x$ at high hydrogen pressure, become *a*-$Tb_{1-y}Fe_2H_x$+Tb_yH_2 at intermediate hydrogen pressure and decomposes directly into TbH_2 and α-Fe at the lower hydrogen pressure [10]. As the temperature increases, TbH_2 precipitate in the amorphous phase and the remaining amorphous phases decompose into TbH_2+α-Fe. The hydrogen content in *c*-$TbFe_2H_x$, which transforms to *a*-$TbFe_2H_x$, is x=4.8. On the contrary, the hydrogen content

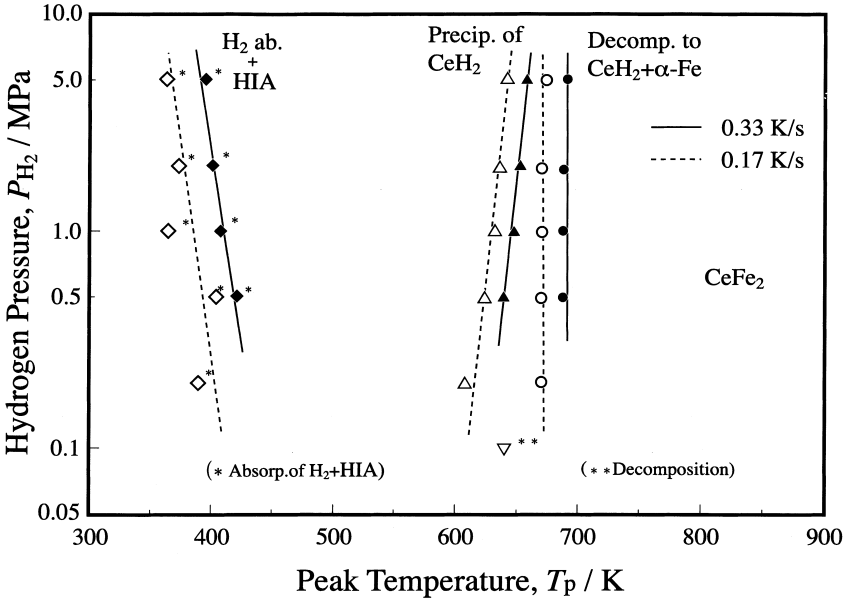

Fig. 5. The peak temperature, T_p, of each reaction against the hydrogen pressure at two heating rates, 0.17 K/s (open symbols and dotted line) and 0.33 K/s (solid symbols and solid line) for $CeFe_2$.

in c-$TbFe_2H_x$, which decomposes into α-Fe+TbH_2, is x=3.6.

4. Discussion

Fig. 5 shows the peak temperature of thermal reactions, T_p, against the hydrogen pressure in $CeFe_2$ for two heating rates 0.17 K/s (open symbols and dotted line) and 0.33 K/s (solid symbols and solid line). Hydrogen absorption and HIA occur simultaneously in $CeFe_2$ independent of the hydrogen pressure. As the hydrogen pressure increases, T_p for HIA and decomposition of the amorphous phase shift to the lower temperature side, which implies that these reactions are controlled by the diffusion of hydrogen or Ce which interacts with hydrogen. On the contrary, T_p for precipitation of CeH_2 shift to the high temperature side, so that precipitation of CeH_2 is not controlled by the diffusion of hydrogen or Ce, but by the diffusion of Fe which does not interact with hydrogen.

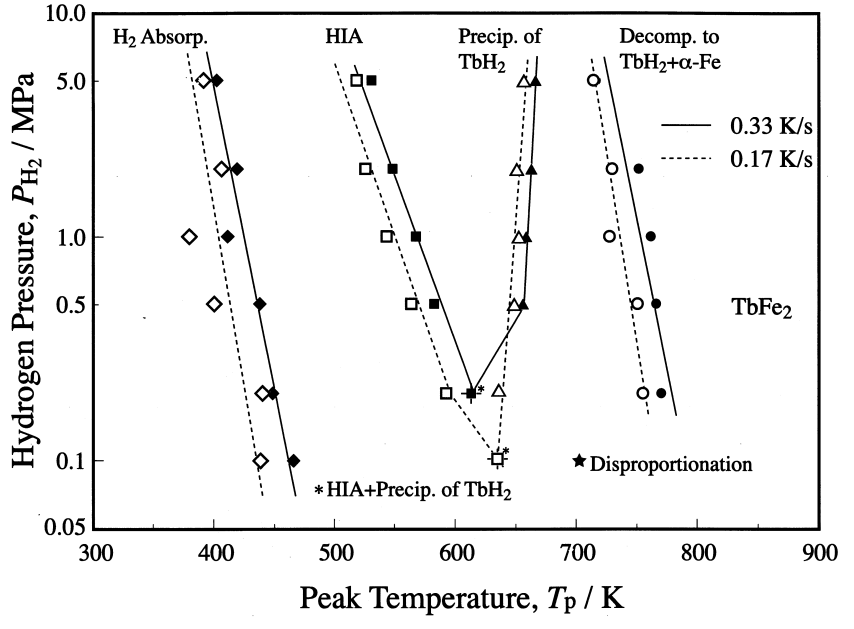

Fig. 6. The peak temperature, T_p, of each reaction against the hydrogen pressure at two heating rates, 0.17 K/s (open symbols and dotted line) and 0.33 K/s (solid symbols and solid line) for $TbFe_2$.

Fig. 6 shows the peak temperature of thermal reactions, T_p, against the hydrogen pressure in $TbFe_2$ for two heating rates 0.17 K/s (open symbols and dotted line) and 0.33 K/s (solid symbols and solid line). As the hydrogen pressure increases, T_p for hydrogen absorption, HIA and decomposition of the amorphous phase shift to the lower temperature side. Consequently, these thermal reactions are controlled by the diffusion of hydrogen or Tb, which reacts with hydrogen in the same way as $CeFe_2$. On the contrary, T_p for precipitation of TbH_2 shift to the high temperature side, which indicates that precipitation of TbH_2 is controlled by the diffusion of Fe atoms which does not react with hydrogen. As a result of these pressure and temperature dependences, HIA overlaps with precipitation of TbH_2 at 0.2 MPa H_2 at 0.33 K/s. On the other hand, no HIA occurs by heating of $TbFe_2$ at 0.1 MPa H_2 and 0.33 K/s. Next, we discuss why HIA occurs above the critical hydrogen pressure. As the hydrogen pressure increases, the amount of hydrogen absorbed in the crystalline phase increases. When the lattice expansion induced by hydrogen atoms exceeds the critical value, the collapse from the crystalline to the amorphous phase may occur. In order to evaluate the critical strain for HIA, in situ XRD experiments are essential. The reason why $CeFe_2$ amorphizes independent of the hydrogen content is explained as follows. Since the atomic size ratio of $CeFe_2$ is large and its melting point is low, it is considered that the stability of c-$CeFe_2H_x$ is lower than that of $TbFe_2$. Consequently, hydrogen absorption in $CeFe_2$ may lead to formation of the amorphous phase.

5. Summary and conclusions

Hydrogen absorption in $CeFe_2$ always gives rise to HIA and no c-$CeFe_2H_x$ hydride is formed under the present conditions. On the other hand, hydrogen absorption, HIA, precipitation of TbH_2 and decomposition of the amorphous alloy into TbH_2 and α-Fe occur exothermally with increasing temperature of $TbFe_2$ above 0.5 MPa H_2. As the hydrogen pressure increases, the peak temperatures of hydrogen absorption, HIA and decomposition of the remaining amorphous alloys shift to lower temperatures, but that of precipitation of TbH_2 shifts to higher temperatures. As a result, HIA and precipitation of TbH_2 overlap each other at 0.2 and 0.1 MPa H_2. HIA in $TbFe_2$ may occur when the lattice expansion by absorbed hydrogen attains to the critical value.

Acknowledgements

This work was supported in part by a Grant-in-Aid for Scientific Research on Priority Areas A of ‘New Protium Function’ from the Ministry of Education, Science, Sports and Culture.

References

[1] K. Aoki, T. Yamamoto, T. Masumoto, Scripta Metall. 21 (1987) 27–31.
[2] L.E. Rehn, P.R. Okamoto, J. Pearson, R. Bhadra, M. Grimsditch, Phys. Rev. Lett. 59 (1987) 2987–2989.
[3] U.-I. Chung, Y.-G. Lim, J.-Y. Lee, Phil. Mag. B63 (1991) 1119–1130.
[4] A.Y. Yermakov, N.V. Murshnikov, N.K. Zajkov, V.S. Gaviko, V.A. Barninov, Phil. Mag. B68 (1993) 883–890.
[5] V.S. Gaviko, V.V. Serikov, N.M. Kleinerman, A.Y. Yermakov, J. Alloys Comp. 284 (1999) 70–76.
[6] K. Aoki, T. Masumoto, J. Alloys Comp. 231 (1995) 20–28.
[7] M. Dilixiati, K. Kanda, K. Ishikawa, K. Suzuki, K. Aoki, J. Alloys Comp. 330–332 (2002) 743–746.
[8] M. Dilixiati, K. Kanda, K. Ishikawa, K. Aoki, J. Alloys Comp. 337 (2002) 128–135.
[9] K. Aoki, M. Dilixiati, K. Ishikawa, Mater. Sci. Eng. A, in press.
[10] M. Dilixiati, K. Kanda, K. Ishikawa, K. Aoki, Mater. Trans. 43 (2002) 1089–1094.